Using Microelectrode Arrays to Explore the Somatosensory System in the Freely Moving Rat

Cognitive Neuroscience MSc Thesis

Han Langeslag

E-Mail: langeslay@hotmail.com

Student number: 0349178

Donders Institute for Brain, Cognition and Behaviour
Radboud University Nijmegen

Supervisors:

Dr. Eric Maris

Date: 01-2010

Abstract

In this paper we describe a new method of chronically obtaining neurophysiological data in the awake and freely moving rat. The method involves placing a flexible microelectrode array (32 electrodes on a 6 by 5 mm polyimide foil) epidurally onto the rats neocortical somatosensory system. Furthermore, we describe a somatosensory discrimination task which we intend to use to study the neurophysiological mechanism behind pattern recognition in the rat as measured by local field potentials from the surface of the neocortex. The new microelectrode array showed relatively artifact free brain signals and is less correlated then extra-cranial EEG recordings. Moreover, using a multiway decomposition method we can unveil a spatial pattern in the ongoing neurophysiological activity of the awake rat as measured by the microelectrode array. The pattern consists of a *phase-amplitude coupling* (PAC) between the phase of a 2-4 Hz oscillatory component and the amplitude of a 30-50 Hz oscillatory component. While we are still in the process of optimizing the methods, we think that the use of polyimide microelectrode arrays will provide an excellent opportunity to chronically study large scale neural activity in the awake and freely moving rat.

1. Introduction

In this paper we will describe a new method of chronically obtaining neurophysiological data in the awake and freely moving rat. This method is particularly suited to study the interactions between different neocortical areas. Studying interactions between neocortical areas is highly important to understand the neurophysiological mechanisms underlying cognition.

One example of a cognitive function of the brain is its ability to recognise familiar sensory patterns. Recognition of familiar patterns allows to see constancy and regularity in the world and to use these regularities to guide behaviour. In order to enable recognition of the same patterns over time memories of these patterns are created and consolidated via changes in synaptic strengths between neurons. These structural synaptic changes lead to a different processing of familiar and unfamiliar sensory stimuli. Therefore, the key aspect behind the understanding of the neurophysiological mechanism behind pattern recognition is to investigate the characteristics of this differential activity.

We use the rat microvibrissae system as a model system to examine this mechanism by obtaining sensory input of the rat's upper lip. This system is used extensively to explore the environment in a tactile manner. Tactile sensory input is particularly important for the rat's phenomenal world, comparable to the visual input for humans. Each of the rat's vibrissae projects via two intermediate synapses to a unique cluster of cells in layer 4 of the primary somatosensory cortex (S1), the so-called barrel cortex (see Figure 1, for detailed descriptions of the rats barrel system see Petersen, 2007).

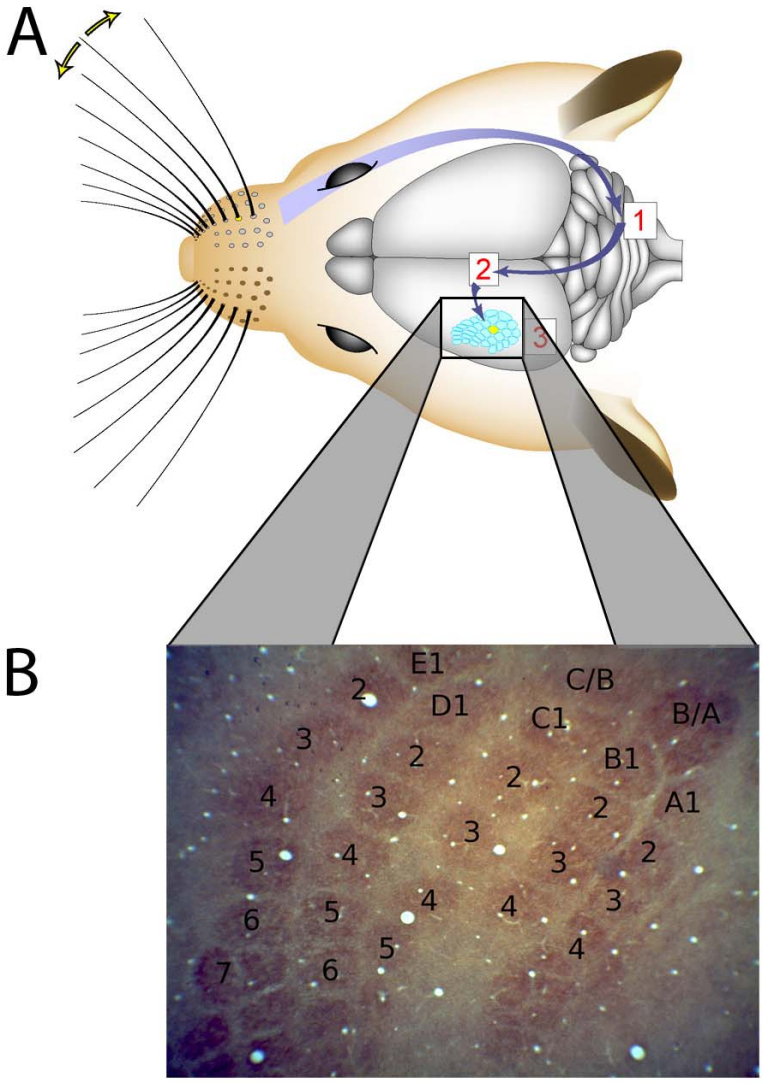

Figure 1. Rat whisker system **A**) From displacement of the whisker mechanoreceptors in the snout send signals to the brain stem (1) Then the signal is transferred to the ventral posterolateral thalamic nucleus (VPL) (2) From there the signal goes to the primary somatosensory cortex; the barrel cortex. Figure taken from Peterson (2007). **B**) The rats barrel cortex for the large whiskers. The dark spots are clusters of cell bodies (Nissl stained piece of neocortex). Each of these clusters, so called 'barrels', corresponds to the input of one of the large whiskers. Furthermore, the barrels are organized in a similar topography as the whiskers on the snout.

Most studies so far have focused on the macro vibrissae of the rat (but see Brecht, Preilowski & Merzenich, 1997), because of relatively easy access to the macro vibrissae and the corresponding barrel cortex. We choose to study the micro vibrissae on the rat's upper lip, since they cannot be moved (whisked) actively by the rat itself, in comparison to the macro vibrissae. Whisking behaviour complicates the interpretation of neocortical brain activity, because it modulates the recorded sensory input in barrel cortex (Ahissar, 2008). Therefore, a higher experimental control would be required by either restraining or measuring the whisking. Furthermore, it is difficult to present complicated tactile patterns to multiple whiskers (but see Jacob, Le Cam, Ego-Stengel & Shulz, 2008).

Because of its somatotopic organisation, the barrel cortex is well suited for studying sensory processing. The micro and macro vibrissae on either side of the rat's nose project unilateral to the contralateral primary somatosensory cortex. From the primary somatosensory cortex the incoming somatic signals are transferred to the secondary somatosensory area (S2) (bilateral). From there the signals propagate to the insula, which is a multisensory area (Rodgers, Benison, Klein & Barth, 2008).

A complicated cognitive task such as pattern recognition most likely involves the synergetic activity of several brain areas. Therefore, the investigation of the neurophysiological mechanism behind pattern recognition (in the somatosensory system) requires the recording of brain activity of large cortical areas. In our case we are interested in the primary and secondary somatosensory cortex and the insula (Rodgers et al., 2008; Frostig, Xiong, Chen-Bee, Kvasnak & Stehberg, 2008).

Furthermore, we would like to record as close to the brain as possible in order to get good signals with a high spatial and temporal resolution. This is imperative to be able to study the dynamics of neural activity in several brain areas at the same time. Therefore, human imaging (fMRI, M/EEG, etc.) methods are not suited for our purpose. Invasive brain data from humans would be ideal but is scarce and comes mostly from epilepsy patients. Recordings in these patients are often made via wire electrodes inserted into the brain or recordings made epidural from the cortical surface using special EEG contacts. This intracranial EEG (iEEG) data has been invaluable in characterizing large scale human brain activity during cognitive tasks (Engel, Moll, Fried & Ojemann, 2005; Jerbi et al., 2009). However, recording sites in epileptic patients are determined on the basis of clinical considerations. Furthermore, these patients are suffering from severe epilepsy and, next to having abnormal brain activity, are constantly in an abnormal health condition. Access to the patient is therefore difficult and cognitive performance is usually below the healthy population average.

A good alternative would be to use a similar intracranial technique in animals. In contrast to human electrophysiology, the field of animal electrophysiology has been dominated by spike recordings from single- or multiunit recording setups. Often, these recording setups have limited spatial coverage because only a limited number of microelectrodes are inserted. However, more recently silicon probes like the Utah array and the Michigan probe (Lakatos, Karmos, Mehta, Ulbert & Schroeder, 2008) have been used and cover larger regions. But, the fact that these techniques are highly invasive, i.e. the electrodes penetrate the cortical layers, limits their chronic use (for a comparison see Ward, Rajdev,

Ellison & Irazoqui, 2009). Moreover, it remains a question how much the neural damage caused by the penetrating electrode influences the neuronal activity recorded.

Recently, some groups recording neuronal activity in monkeys have made use of grids similar to those used in iEEG recordings in humans (Taylor, Mandon, Freiwald, Kreiter, 2004). However, research in monkeys is often restricted in terms subjects numbers and genetic possibilities. Therefore, having a similar method in rodents would be advantageous. Other groups have already made use of non-penetrating wire-electrodes arranged in array form placed epi/sub-dural in rats, gerbils and rabbits (Benison, Rector & Barth, 2007; Rodgers et al., 2008; Ohl, Scheich & Freeman, 2001; Barrie & Freeman,1996). These arrays could be implanted chronically, but the movement of the animal was often restricted and/or cortical coverage was limited.

Recent advances in retinal implants have made it possible to make miniature electrode grids onto a flexible polymer (for instance polyimide). Now several research groups have used these techniques to record brain signals or stimulate the motor cortex in rodents (Hollenberg, Richards, Richards, Bahr & Rector, 2006; Molina-Luna et al., 2007). However, these experimental setups were not intended for chronic recording in behaving animals (but see Rubehn, Bosman, Oostenveld, Fries & Stieglitz, 2009 for monkeys). Moreover, most of these recordings were performed under anaesthesia.

In our study, we make use of a similar microelectrode array as used by Molina-Luna et al. (2007). By using such an array, we are not able to obtain spike data, but we have a method of recording similar to human iEEG recordings. In humans these recordings have proven useful in characterising large scale brain activity and in particular oscillatory interactions between brain areas (Varela, Lachaux, Rodriquez & Martinerie, 2001; Canolty et al., 2006). We believe that the use of these arrays makes a good compromise between spatial resolution and cortical coverage, while at the same time being less invasive than penetrating electrodes.

We aim to characterise the means by which the rat's somatosensory cortex interact during the presentation of tactile patterns. The presented patterns will be either recognisable or not. This will be accomplished be presenting completely novel patterns next to learned patterns or by presenting incomplete learned patterns. In this study we look at coupling between amplitude envelopes and phases at different frequencies (Canolty et al., 2006, Doesburg et al.,2009) and correlations between frequency envelopes (Bruns & Eckhorn, 2004). In particular we intend to look at the difference in these variables when presenting learned patterns, novel patterns or incomplete learned patterns. This way we can study vibrotactile pattern recognition in the rat's somatosensory system.

2. Materials and methods

2.1 Microelectrode array

The microelectrode array consisted of 36 Titanium Nitrite (TiN) contacts; 32 electrodes with a diameter of 480 µm and 4 electrodes that functioned as grounds and references. The electrodes were placed on a sheet of 14 µm thick polyimide foil. The polyimide foil was strong and highly flexible, making it ideal to follow the surface of the cortex. The current that entered and left the TiN contacts flowed over insulated gold lanes that were integrated in the polyimide foil and ended in a connector piece (see microarray on Figure 2). The materials from which the microelectrode array was made of have proven to be highly biocompatible (Hämmerle et al., 2002).

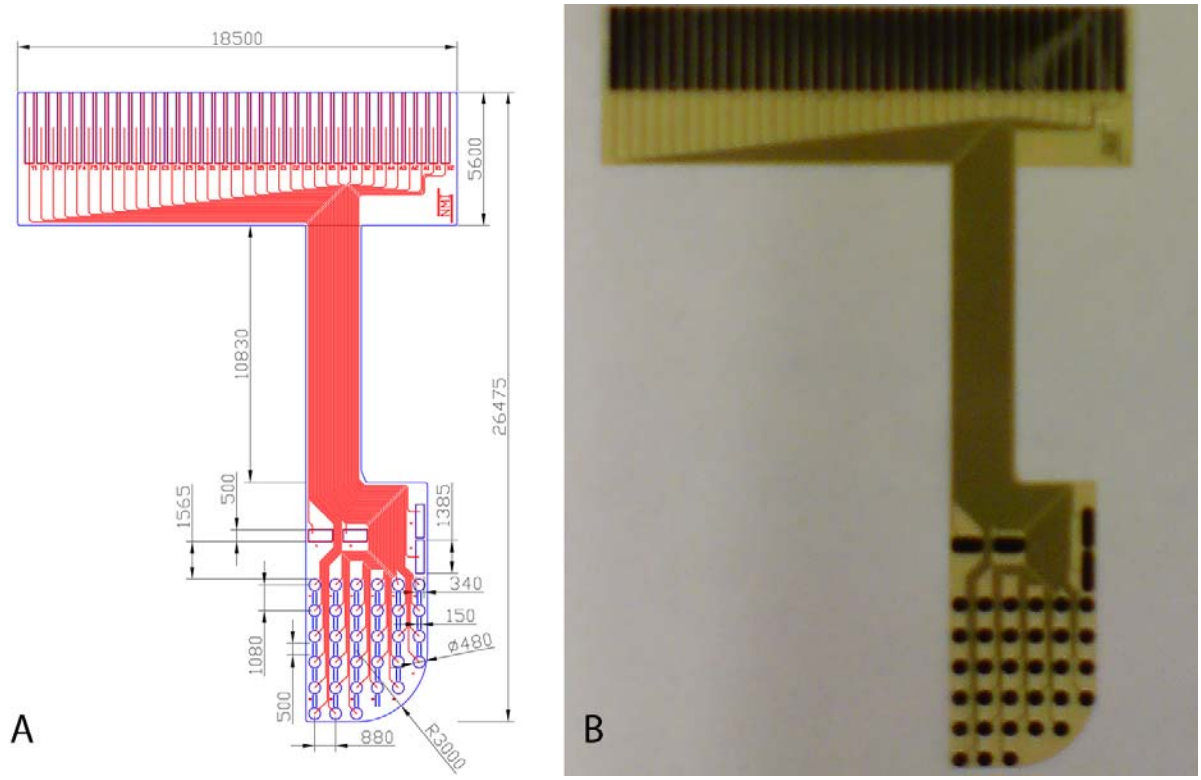

Figure 2. A) Left hemisphere array design (looking against the contact surfaces). Blue rounds are the 32 channels, the four rectangles are the grounds and reference electrodes. The red lines are the gold wires which end up in the connector piece of the microarray, given by the 36 small rectangular contacts. **B**) The actual array for the left hemisphere. Contacts are in black.

Although we did not measure the impedance of our electrodes in vivo, we expected it to be around 9 kΩ. This value was calculated from impedance measurements performed by Hosp et al. (2008). The TiN contacts were determined by Hosp et al. (2008) to have an

average impedance of 198±68.9 kΩ at 1 kHz. However, the used contact diameter in that study was only 100 µm; our electrodes were almost five times larger in diameter. Assuming a linear drop-off with increasing electrode surface, the surface area of our electrodes increased with more than a factor of 23, thereby reducing the average impedance to 198/23 ≈ 8,6 kΩ.

The microarray was designed to cover most of the rat somatosensory system. Based on the rat brain atlas of Paxinos & Watson (2007), we designed an array of 5 x 6 mm. Figure 3 shows the approximate coverage of the array on the cortical surface.

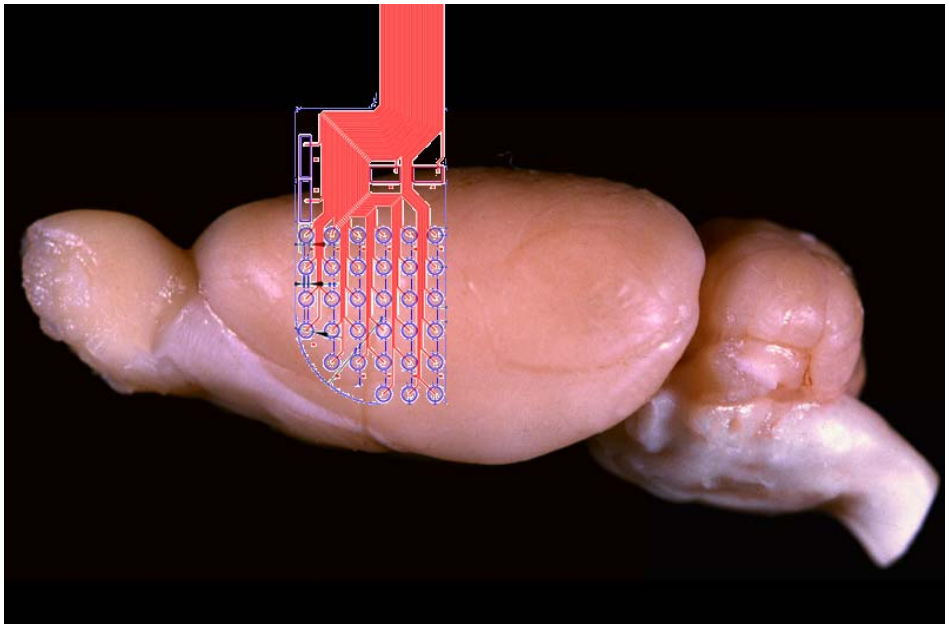

Figure 3. Approximate coverage of the array on the left hemisphere of the rat.

Two arrays were designed to cover either the left or right hemisphere. Furthermore, the design was such that arrays could be implanted bilaterally. The microarrays are commercially available from NMI (NMI, Reutlingen, Germany). In Figure 4 the red line on the coronal cross-section indicates the estimated coverage of the rat's somatosensory cortex.

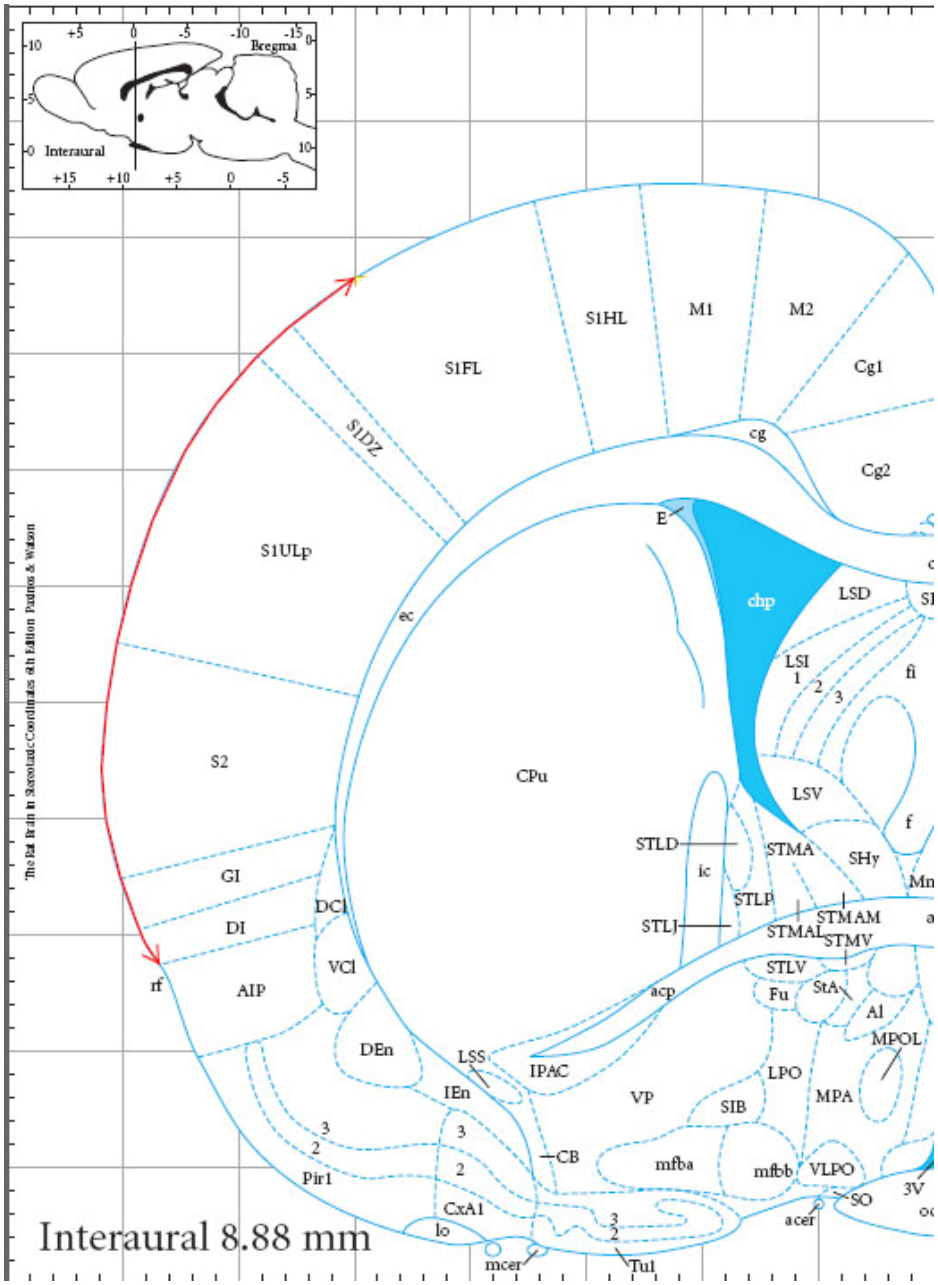

Figure 4. The red line on this coronal cross-section indicates the targeted coverage of the microelectrode array. Important are S1ULp (primary somatosensory cortex of the upper lip), S2 (secondary somatosensory cortex), GI (granular insula) and DI (disgranular insula).

2.2 Surgical procedures

The surgical implantation of the electrode array was done in two steps to allow the skull bone to heal in between the two surgeries (See Figure 5 for the complete surgical set-up). We chose to let the skull bone heal to minimise the risk of infection and thereby increasing the lifetime of the animals. The first surgery involved the making of a craniotomy, the placement of the microelectrode array, and the replacement of the skull bone. The second

surgery involved the attachment of a recording chamber to the rat's skull in order to connect the polyimide connector to a circuit board via a zif connector. After each surgery the animals were housed individually and maintained on a 12 hour light/dark cycle with lights on during the night. The experiments were approved by the Ethical Committee on Animal Experimentation of the Radboud University of Nijmegen, The Netherlands.

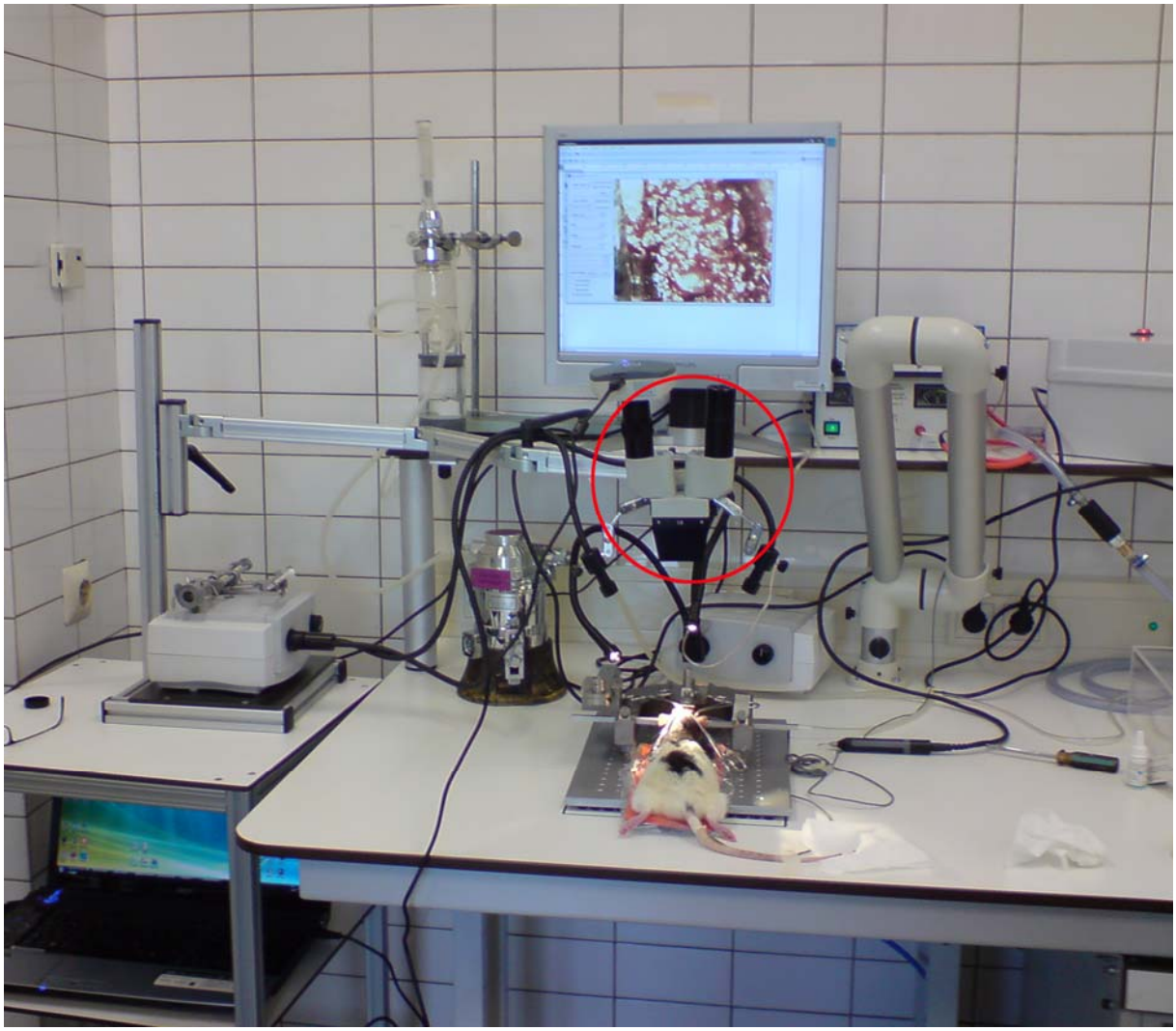

Figure 5. Surgical setup (without piezodrill). Encircled in red is the microscope with a USB camera which displays the surgical working area on the monitor above.

2.2.1 Array implantation

Five Long Evans rats (3 months old, 450-500g body weight, Harlan, USA) were implanted with a microelectrode array, four with a right hemisphere array and one with a left hemisphere array. We placed the array over the somatosensory system, in particular the part that processes the incoming signals from the microvibrissae. The target area of cortical surface is located on the lateral part of the rat's brain. This area is not easily accessible

because it lies under the rat's jaw muscles. We therefore did not want to remove the bone directly on the side of the skull in order to keep the jaw muscles tissue intact. Instead we made a craniotomy of 8 x 4 mm (see Figure 6a for intended placement of the electrode array via the craniotomy). The craniotomy was made with a piezoelectric drill (PiezoSurgery, Mectron s.p.a., Carasco, Italy) using a blunt round drill head (1 mm in diameter). We chose piezosurgery over conventional mechanical drills, because it is particularly save for soft tissue. The piezodrill only cuts through hard material like bone, but not through soft tissue like the brain and the dura mater.

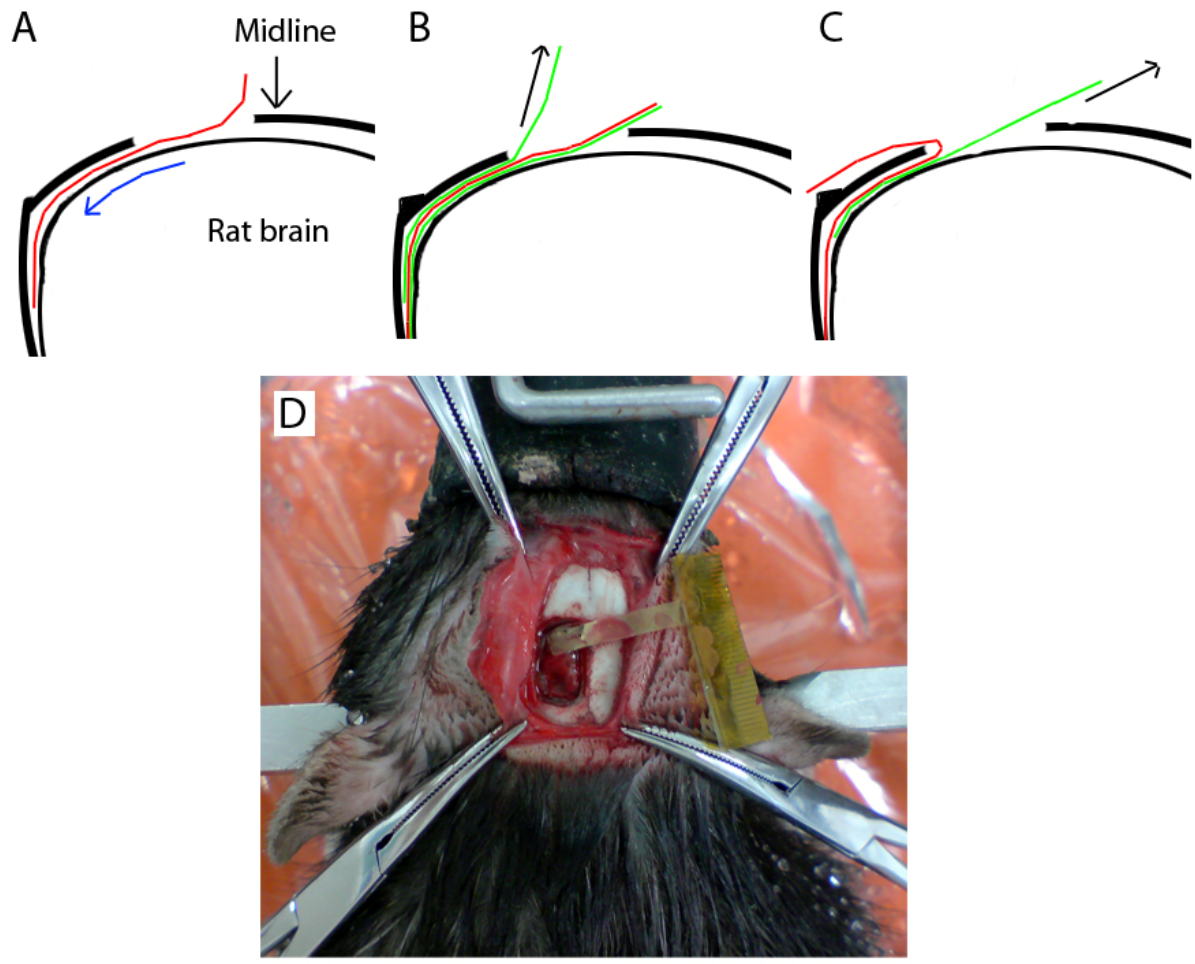

Figure 6. Array placement, array in 6A-C is the red line, the thick black line is the skull bone, the thin black line is the brain contour. In 6B-C the messing strips are shown in green. **A**) The array is placed in between the skull and the brain, the array is pushed down to the lateral side (direction of the blue arrow). **B**) Extraction of the top messing strip. After placement of the array the top strip is removed first in the direction of the black arrow. **C**) Next the bottom messing strip is removed in the direction of the black arrow while the array is flipped over to the lateral side. **D**) Result after successful placement. This is the final position of the array before the craniotomy is filled with TCP granules.

Rats were anaesthetized by means of Isoflurane. Depth of anaesthesia was monitored throughout the surgery by checking if the toe reflex could be elicited. Lidocaine (2 % plus adrenaline) was used as a local anaesthetic after the initial incision was made and while scraping the periost to the sides. While anesthetized, the rat was placed into a standard stereotactic device. Preoperatively, we administered atropine (0.2 ml, i.m.), which improves respiration during surgery, and Rimadylmix (1:5 Rimadyl:NaCL, weight-dependent dosage, s.c.), an analgesic. Temperature was kept at the rat's initial body temperature (between 36 and 37 degrees Celsius as measured with a rectal thermometer) via an automatically regulated heating pad. Because of the piezodrill's water-cooling sometimes an extra red light breeding lamp was used to maintain the rat's body temperature after long periods of drilling. Furthermore, to avoid excessive cooling of the rat's body temperature and to maintain a dry workspace, we used a custom made small vacuum pump.

The initial incision going from the eyes to a position slightly posterior to the ears exposed the periost. The periost was cut over the midline and scraped to the sides thereby exposing the skull bone. The bregma was determined and the corners of the subsequent craniotomy were marked.

The piezodrill was used to cut through the bone. While drilling we checked the position within the skull bone in order to prevent a damage of the dura. It is only 80 micron thick and therefore easy to tear. We lifted the respective piece of skull carefully. Since the dura sticks to the skull bone, we needed to separate the two from each other. To do this as careful as possible, we used a small dental excavator to slowly scrape the dura of the skull bone.

Next, the array was inserted underneath the bone to the lateral side. It was 'sandwiched' between two messing strips (each 25 micron thick), because it was too thin to be pushed down the lateral side without folding. The top messing strip was removed, after the final position was reached (Figure 6b). The part of the array that stuck out over the lateral side of the rat's head was moved to the opposite site to be able to remove the underlying piece of messing (Figure 6c). Afterwards, the array was moved to the opposing side again, covering the craniotomy (Figure 6d). On top of the array and the exposed dura we filled the cavity with Tri-calcium phosphate (TCP, Conduit TCP granules, DePuy International LTD, Leeds, UK) granules mixed with autologic blood. This mix of TCP and autologic blood promotes osteointegration (Cao & Kuboyama, 2009). The array connector piece was again folded back over the craniotomy, such that the whole array piece was lying flat over the skull. The skin

was then pulled back over the array and sutured to allow healing of the removed piece of skull bone.

2.2.2 Recording chamber placement

The microelectrode array has to be connected via a zif connector, which is connected to a circuit board. On top of the circuit board an Omnetics connecter (Omnetics Connector Corporation, Minneapolis) serves as the connector to the pre-amplifier (Figure 7a). In order to connect the circuit board to the fragile array's connector piece we needed to place a recording chamber on top of the rat's skull. A titanium rectangular shaped basket (Figure 7b) was bolted to the skull by four screws (Figure 7c). The basket shaped recording chamber was filled up with FLOWline (Heraus-Kulzer, Dormagen, Germany) except for the space above the craniotomy, which was filled up with liquid silicon, Kwiksil (WPI, Sarasota, USA); it is better suited for the underlying soft tissue (Figure 7d).

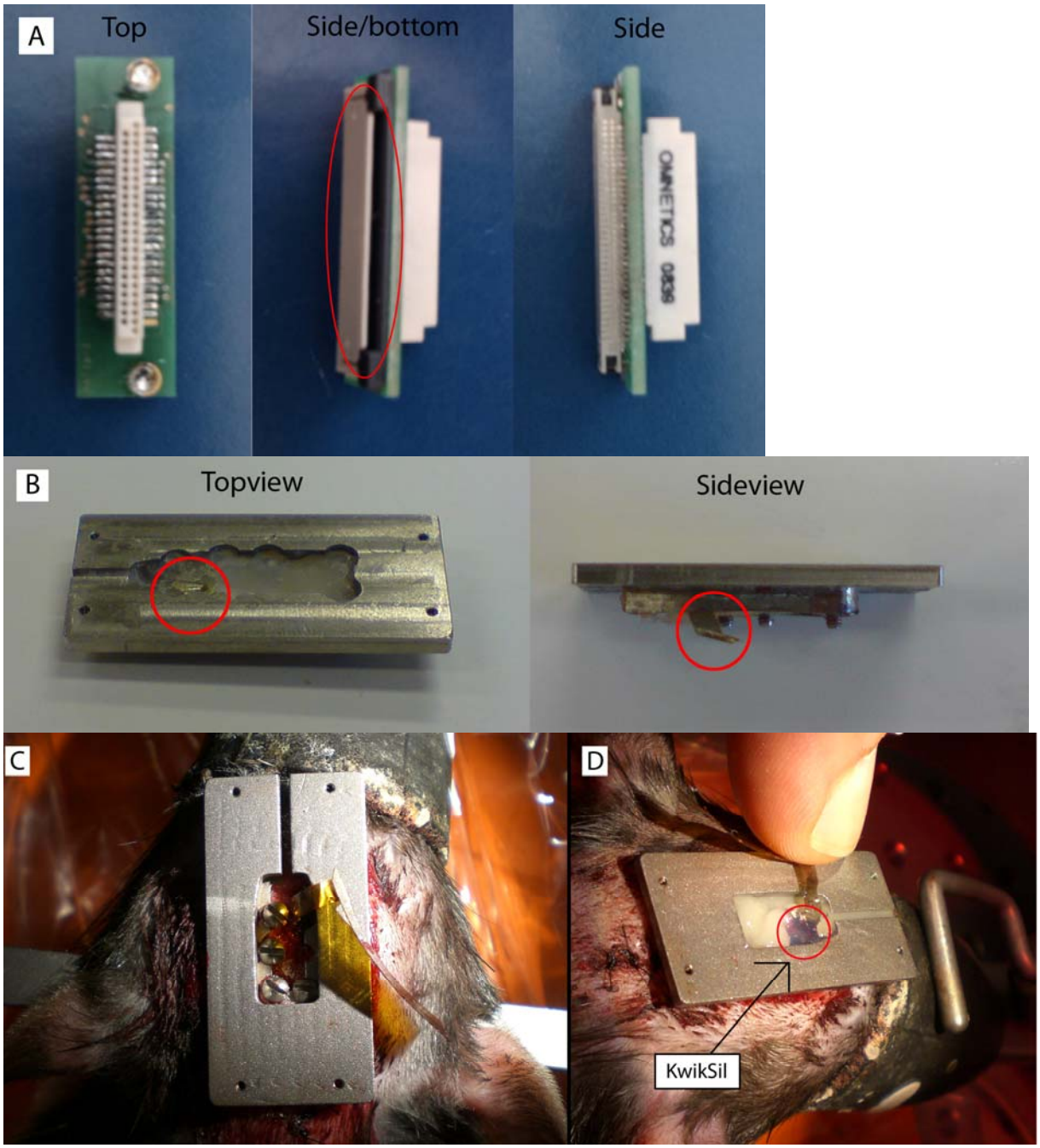

Figure 7. A) Circuit board with zif and Omnetics connector to be attached on top of the recording chamber. The top view shows only the Omnetics connector. Encircled in red is the zif connector into which the connector piece of the micro array is inserted. **B**) Titanium recording chamber (this is a used one). Encircled in red is the cable of the micro array. **C**) Titanium recording chamber seen from above (older model as in **6B**), the top of the picture is anterior. The four screws are clearly visible in this picture. The yellow/gold piece is the connector piece of the array and the cable running to it. The four holes in the corners of the recording chamber are for later attachment of the circuit board and the connector for the pre-amplifier. **D**) The recording chamber seen from above, the right of the picture is anterior. The recording chamber is here filled up with Flowline (white) and Kwiksil (purple). The yellow/gold piece is the cable of the array.

Next, the connector piece was connected to the circuit board and attached to the recording chamber; this provided a connection to the pre-amplifier. Later, it was possible to

tighten the pre-amplifier to the recording chamber by two screws (i.e. as necessary during recordings). The final result can be seen in Figure 8.

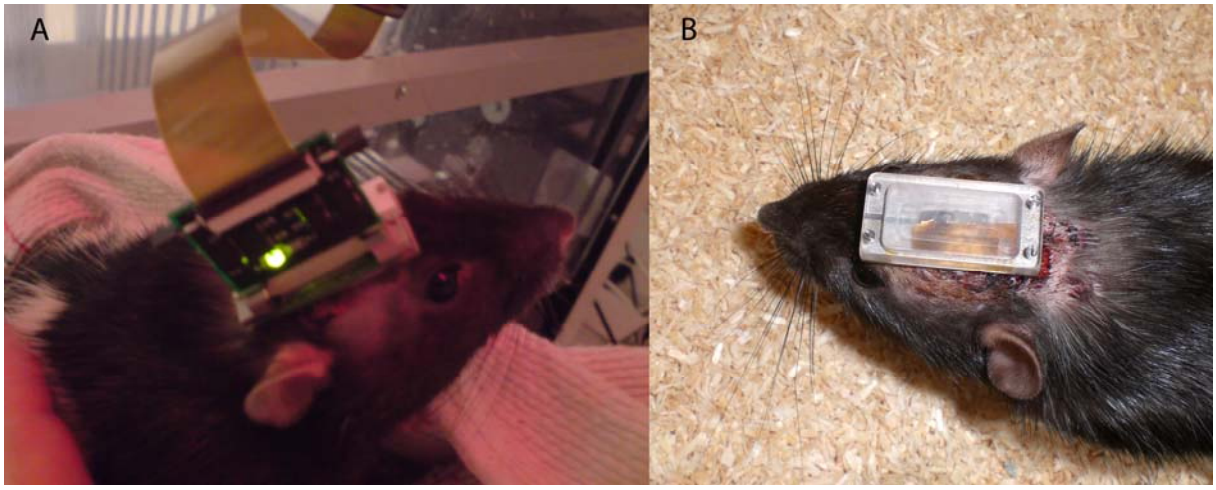

Figure 8. A) Rat connected to the pre-amplifier (circuit board with green LED). **B**) Rat just after the surgery of recording chamber placement. Here the circuit board connecting to the connector piece is not yet attached. Instead a Plexiglas cover is temporarily in place.

2.3 Behavioural training

In order to examine the neurophsyiological mechanism of pattern recognition with respect to the microvibrissae system, we used two Braille stimulators (Figure 9a). These Braille stimulators stimulated the rat's upper lip with vibrotactile patterns. The eight pins of each Braille stimulator could individually be moved up and down with a maximum frequency of 30 Hz. Thus, we were able to apply different patterns of stimulation by moving each pin up and down individually. Vibrotactile stimuli were produced by presenting the tactile patterns at a particular frequency (instead of moving the pins up and down only once). These vibrotactile patterns generate steady-state somatosensory evoked potentials (SSEPs) in S1.

Generally, rats can be trained to fixate their snout for a certain amount of time in a nose-poke hole. We used a laser diode to detect whether the rat covered the nose-poke with the tip of its nose. During this fixation, vibrotactile patterns were presented to the upper lip. After stimulation, the rat was rewarded by sugar water in one of two cups (left or right). These cups contained a laser diode to detect the licking response. The complete set-up is shown in Figure 9b.

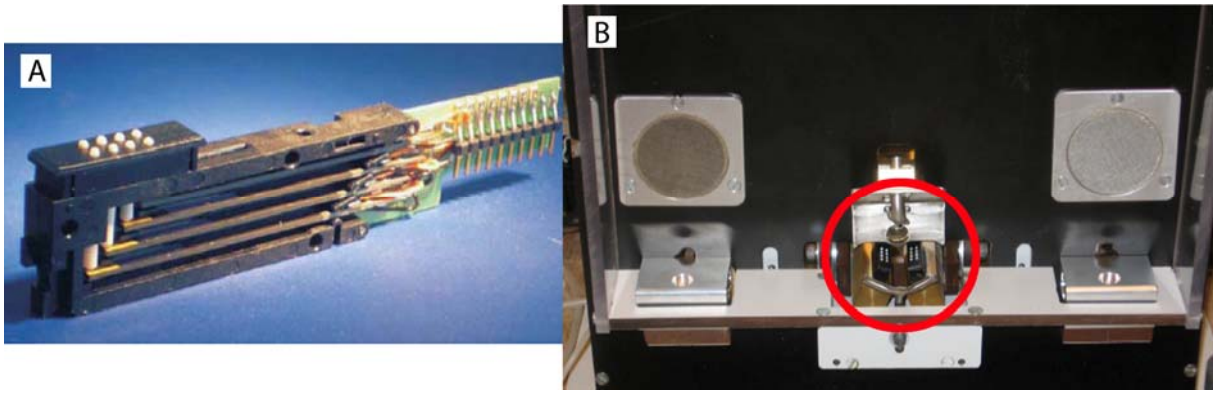

Figure 9. A) Braille cell. The eight white dots are the endings of eight pins that can be moved up en down independently. **B**) Complete setup, the rat has to put its nose in between the two Braille cells (two black rectangles on top of the copper elements in the in the red circle) and in the nose-poke hole that is in between the Braille cells. In the left and right lower corners there are two reward cups for sugar water. Above the reward cups are two speakers to indicate the onset of the reward dispense for the rat.

2.4 Recording setup

Recordings were made with a DigitalLynx10S (NeuraLynx, Montana, USA) signal amplifier system. Data was collected via Neuralynx Cheetah software. Recordings were sampled at 2, 4 and 8 kHz and high pass filtered at 0.1 Hz to avoid slow drifts in the signal. Data was stored for subsequent offline analyses.

2.5 Data analyses

The goal of the performed data analysis was to identify patterns in the ongoing neurophysiological activity as measured by the cortical surface LFP's. The continuous data recorded in Neuralynx was converted into Matlab 2008b (Mathworks, Natick, MA). Within Matlab a large part of the subsequent analysis was performed with the Fieldtrip toolbox developed at the Donders Institute for Brain, Cognition and Behavior (http://fieldtrip.fcdonders.nl/). We combined the Fieldtrip Toolbox with the N-way Toolbox developed by Andersson & Bro (2000) (http://www.models.kvl.dk/source/) to perform the tensor decomposition analyses.

2.5.1 Preprocessing

The raw continuous data was checked for heartbeat artifacts, since there are a lot of large veins in between the cortical surface and the electrode array. PCA decomposition was

performed, but none of the components of the PCA output resembled a heartbeat (i.e. 300-400 beats per minute for a rat).

Next, the continuous raw data was cut into segments of 3 s. All segments were visually inspected for artifacts (e.g. segments containing sharp spikes were removed). Before any further analyses were performed the segmented data was DFT filtered at 50, 100, 150 and 200 Hz to remove the present 50 Hz linenoise and the first three harmonics. The DFT filter consisted of a notch filter set at 50, 100, 150 and 200 Hz. The notch filter fitted the sine and cosine at the specified frequency to the data and subsequently subtracted the estimated components.

2.5.2 Correlations of raw data and amplitudes

First, the raw data was correlated between channels (averaged correlation between the used segments) to characterise the spatial extent over which electrophysiological activity was measured. Second, to characterise other correlated structures in the data correlations between amplitude envelopes for a set of pre-defined frequency bins were calculated. These amplitude envelopes were obtained by taking the absolute values of the Hilbert transform of each of the bandpass filtered signals. Envelope correlations were calculated with a zero time lag, as well as with 10 steps of 10 ms shifts; there might have been a delay from signals travelling between channels (Bruns, 2004). Positive correlations between (time-shifted) amplitude envelopes index co-occurring bursts of oscillatory activity, which may or may not be phase-consistent (Bruns & Eckhorn, 2004; Ohl, Scheich & Freeman, 2001).

2.5.3 Power spectra

The segmented data was used to calculate the power spectrum using multitaper estimation with orthogonal Slepian tapers (Percival & Walden, 1993; Mitra & Pesaran, 1999). For the frequencies from 1-30 Hz we used 1 Hz frequency smoothing and for the frequencies from 30 to 400 Hz we used 10 Hz frequency smoothing. The power spectra were averaged over segments. Depending on the dataset we used 30 to 100 segments.

2.5.4 Frequency couplings between channels

Furthermore, we performed tensor decomposition on a 4-dimensional array of the data, i.e. channel by channel by phase by frequency. This decomposition was performed to identify the spatial and the frequency spectra that characterise patterns of cross-frequency coupling. In particular, we were interested in the coupling between the phases of low

frequency oscillations and the amplitudes of high frequency oscillations, the so-called *phase-amplitude coupling* (PAC). PAC has been previously identified in rats, cats, monkeys and humans (Sirota et al., 2008, in rats; von Stein, Chiang & König, 2000, in cats; Schanze & Eckhorn, 1997; Lakatos et al., 2008, in monkeys; Bruns & Eckhorn, 2004; Canolty, et al., 2006; Maris, van Vught & Kahana, submitted, in humans). The decomposition method that identifies these spatial and frequency spectra is described in detail by Maris, van Vugt and Kahana (submitted). The method extends on earlier proposed tensor decompositions of electrophysiological datasets (Miwakeichi et al., 2004; Morup et al., 2006) by adding a complex valued tensor decomposition to deal with phase relations between neuronal signals.

First, the raw data to be represented in a complex valued signal representing the time varying amplitude and phase was required. We obtained this representation via a wavelet transform (see Bruns, 2004 for more methods) from which we obtained the amplitude and phases for specific frequency bins as specified by the used set of wavelets. Second, we obtained a coupling strength of couplings between phase and amplitude by a weighted phase-locking factor (wPLF). This wPLF is the covariance of the amplitude envelope of one signal with the (normalised) wavelet transform of the same or another signal. This covariance can be computed for different channel pairs and different frequency pairs. For example, this could be the covariance between the channel 1 phase for frequency bin 3-4 Hz and the channel 2 amplitude envelope for frequency bin 30-50 Hz.

Finally, the wPLFs were put into a 4-dimensional array consisting of: (1) the channels from which the amplitudes were estimated, (2) the channels from which the phases were estimated, (3) the frequency bins of the amplitude estimates, and (4) the frequency bins of the phase estimates. This array was decomposed as a tensor product of (1) the spatial spectrum of the phase-modulated high-frequency amplitude envelope, (2) the frequency spectrum of this phase-modulated high-frequency amplitude envelope, (3) the spatial spectrum of the common slow oscillation that modulates the high-frequency amplitude envelope, and (4) the frequency spectrum of this common slow oscillation (Maris et al., submitted)

The tensor decomposition is an extension of popular bilinear methods such as ICA or PCA decomposition. However, these bilinear models provide non-unique solutions, and therefore constraints need to be applied to attain uniqueness (like orthogonality in PCA, see Shlens, 2009). These constraints are not based on biologically plausible assumptions. Contrary to the bilinear models, a tensor decomposition of a three- or higher-dimensional array gives solutions that are unique up to scaling and permutation without needing strong constraints (Bro, 1998).

3. Results

3.1 Surgical protocol and animal behaviour

After surgical procedures performed as described above, we were left with one rat we were able to record from. One animal died during the first surgery (array placement), one during the second (placement of the recording chamber), one had a broken connector, and one died as a result of a faulty anaesthetic device while making small adjustments to the recording chamber.

3.1.2 Evaluation of tissue integrity

We hoped that the TCP granules would ensure complete healing of the bone. Unfortunately, all four rats that successfully recovered from the first surgery showed no signs of bone reintegration. However, the site of the craniotomy did lock clean and was covered with soft scar tissue in all rats that underwent the second surgery.

To see whether our method of implanting the array to the lateral side was successful we performed a full skull lift on a rat that died early. As shown in Figure 10 the array is in place on the lateral side, i.e. unfolded and undamaged. Lifting of the array itself revealed that the array made good contact to the brain surface. Histological assessment of cortical damage is still pending.

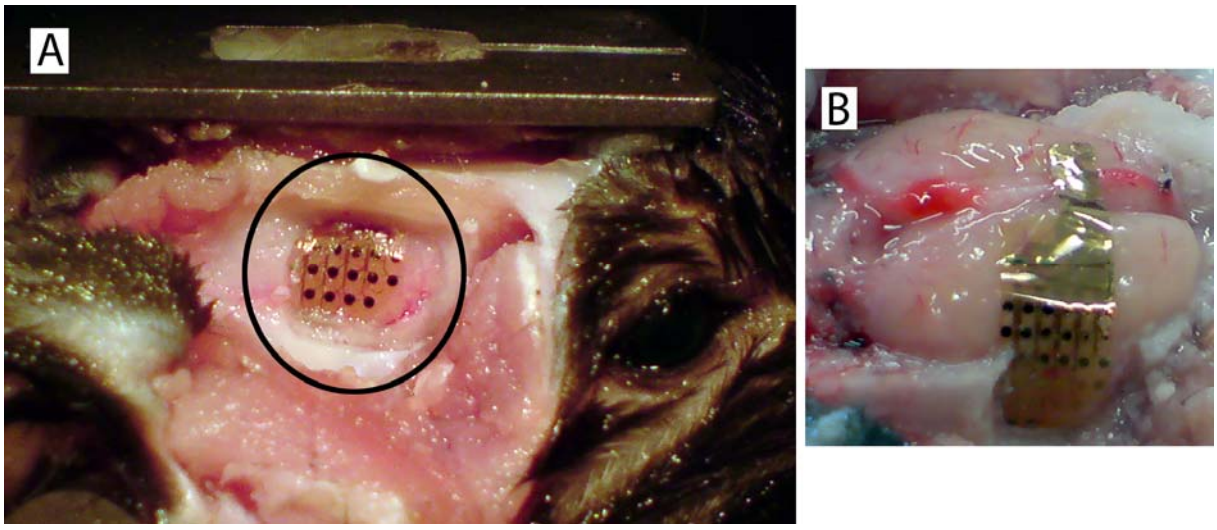

Figure 10. A) Side view of the rat, anterior is to the right (the recording chamber can be seen on top) Placement of the array on the lateral side is clearly visible after a craniotomy on the right lateral side of the rat. **B**) Position of the array on the cortical surface as seen from the top after a complete skull lift, anterior is to the right.

3.1.3 Evaluation of animal behaviour

Unfortunately, we could only make recordings from the rat that survived all surgeries for about a week, because the rat removed the recording chamber by pushing against it with its neck. This problem started when we elongated the recording chamber, which was necessary to add two screws. By means of these screws we could connect the headstage without applying force onto the skull.

During the successful recording sessions, the animal was either sitting still or quietly moving around, i.e. the animal did not perform the behavioural task. To the best of our knowledge, the rat was not sleeping during recordings. Therefore, the data we obtained was continuous (durations of 60 to 1000 seconds) and did not contain any epochs of stimulation. Having no functional mapping by recording SSEP's available (as in Rodgers et al, 2008), we were not able to determine the exact location of the array in terms of cortical regions.

3.2 Evaluation of data quality

Out of the 32 active channels we were able to obtain signals from 29 channels. Hardware continuous signal channel CSC20 (in this paper referred to as channel 31) had a malfunction in the amplifier and therefore gave no signal. Hardware channels CSC32 and CSC31 registered the exact same signal due to a short circuit; therefore, CSC32 was not considered in the further analyses (channel 32 in this paper). Furthermore, we accidently used a circuit board meant to connect to a right hemisphere array. So the signal of CSC19 was actually coming from a ground electrode, which was positioned over the motor cortex. Due to this, CSC19 (channel 30 in this paper) was also excluded from all further analyses.

The raw data contained some artifacts. Especially the abrupt head movements and intensive head washing seemed to cause artifacts on all channels. One of the continuous datasets contained a sharp spectral line at 116 Hz and another dataset showed a sharp spectral line at 11 Hz (isolated by setting the frequency smoothing of the high frequencies to 0.5 Hz). We assumed that these spectral lines in the power spectrum were caused by external noise.

3.3 Correlations between DFT filtered channel data

After DFT filtering the data only showed high correlations in channels 9, 24 and 25 (Figure 11). Figure 12 shows the average of the absolute Pearson correlation coefficient between channels set against the channel distance. The considered distances range from neighbouring channels to a maximum of five channels. Average correlations set against channel distance did not reach 0.3.

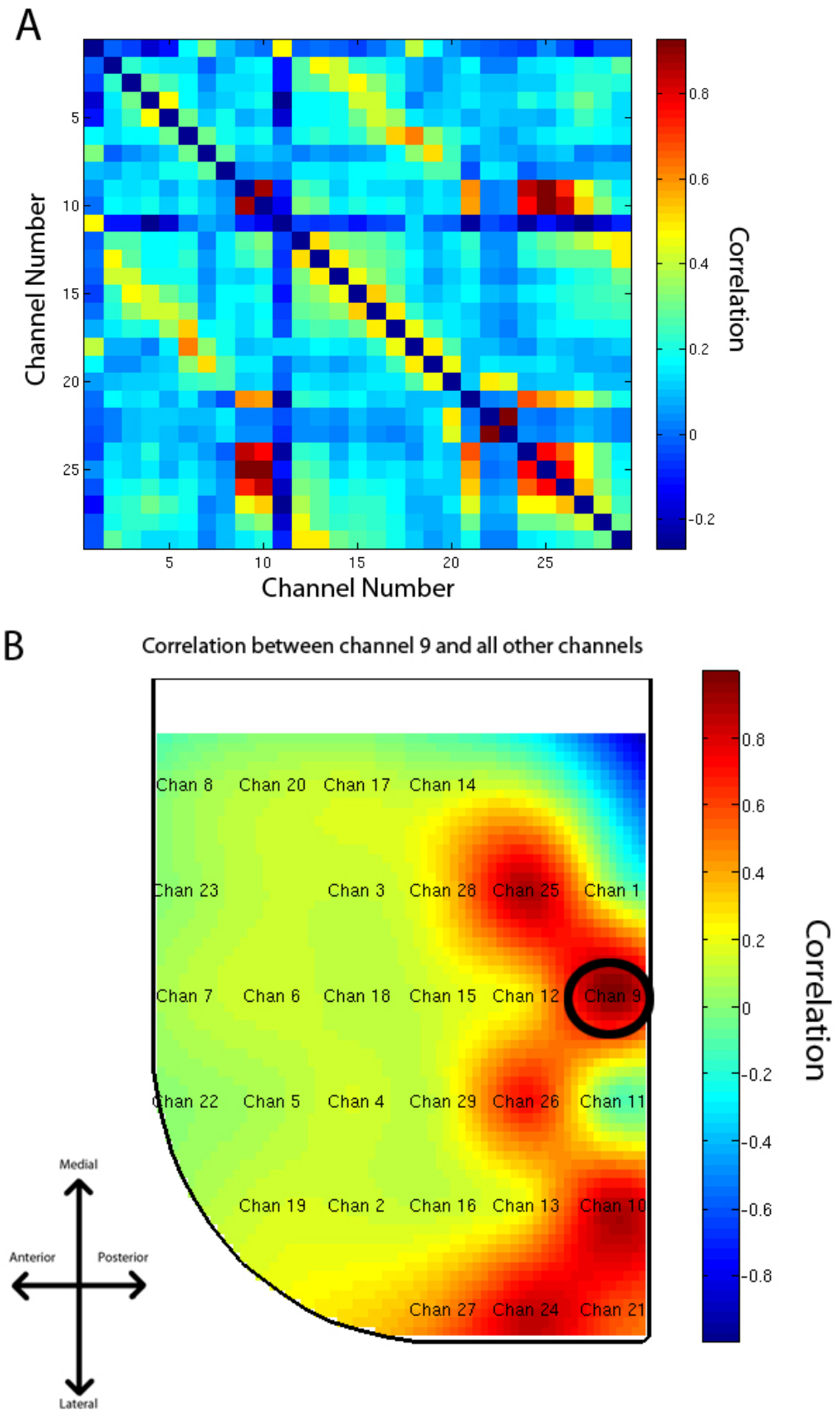

Figure 11. A) Correlations between the raw signal of all 29 channels. **B**) Spatial topography of the correlation between channel 9 and all other channels.

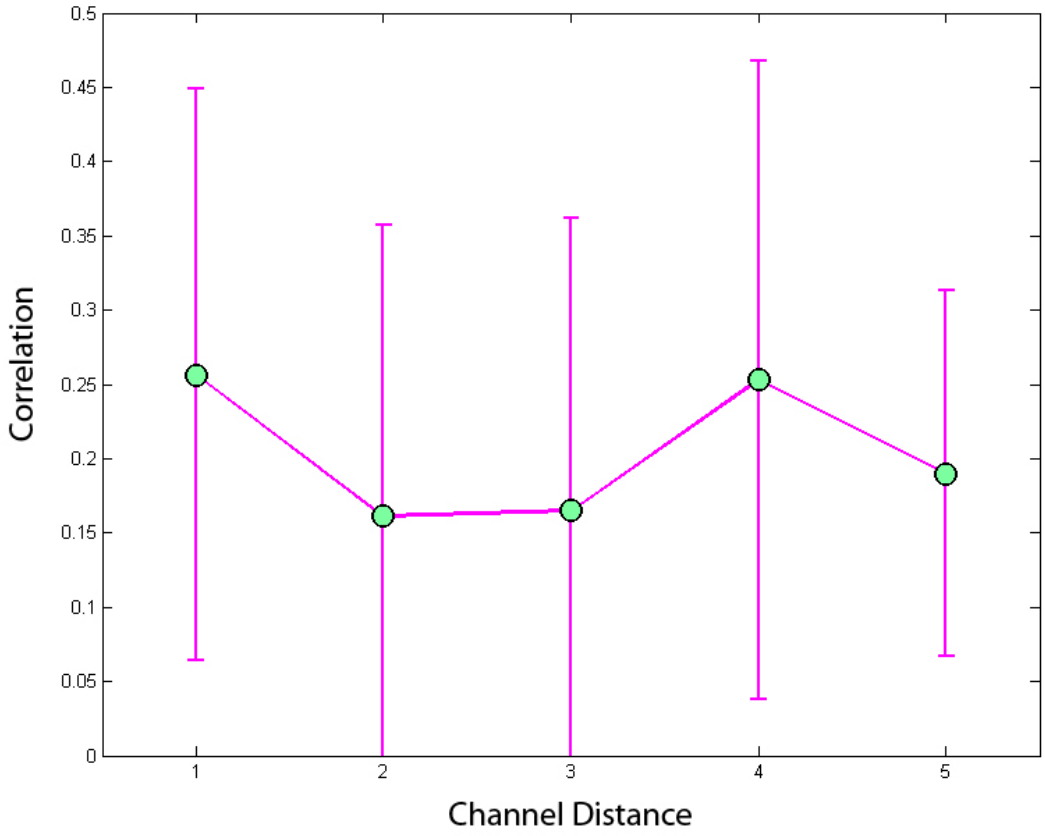

Figure 12. Average Pearson correlation set against the channel distance. Distance runs from 1 channel to 5 channels away. Neighbouring channels distances: 0,88 to 1,393 mm. 2 channel distances: 1,76 to 2,786 mm. 3 channel distances: 2,64 to 4,18 mm. 4 channel distances: 3,52 to 5,572 mm. 5 channels distances: everything above 6 mm.

3.4 Amplitude envelope correlation

The correlation between amplitude envelopes between different channels showed no correlation above 0.2. Time shifting the signals in steps of 10 ms only led to a reduction of this correlation. A weak correlation of 0.28 was observed between neighbouring channels 29 and 26 in the higher frequency bands (i.e. relative to the near zero correlations between the rest of the channels). However, these two channels also showed a high degree of correlation in the raw data.

3.5 Power spectra

The frequency spectra did not show distinct peaks in any frequency band (1 to 400 Hz). The lower frequencies contained the most power, showing a typical 1/f drop-off with

increasing frequency. We show the trial-averaged power spectra for the lower frequencies in Figure 13a and those for the higher frequencies in Figure 13b. All individual channels showed similarly shaped frequency spectra.

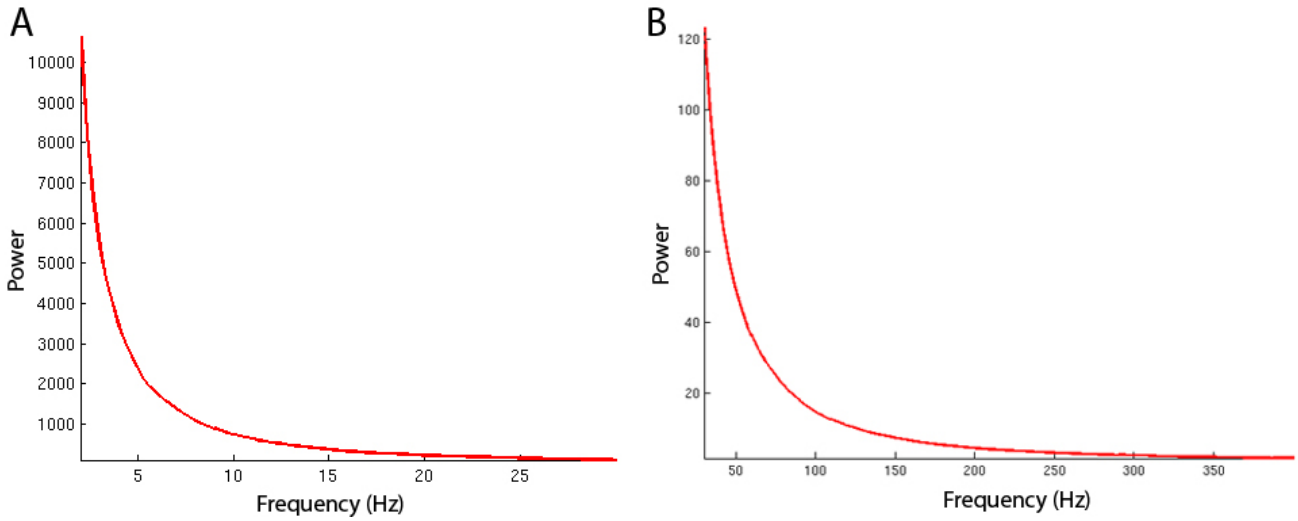

Figure 13. Power spectra, average over 29 channels. **A**) 2 to 30 Hz spectrum. **B**) 30 to 400 Hz power spectrum.

3.6 Phase-amplitude coupling

A tensor decomposition on the four dimensional array of channels by channels, frequency by phase was performed. We found delta frequency band phase (3-4 Hz) to be coupled to gamma frequency band amplitude (30-50 Hz) (Figure 14a shows an example of the coupling between two channels). Thus, bursts of neuronal activity in the gamma band were phase-locked to the slow delta rhythm. Interestingly, only one channel clearly exhibited this delta phase-locked gamma component (Figure 14b). The spatial topography of the delta component, however, was widespread (Figure 14c).

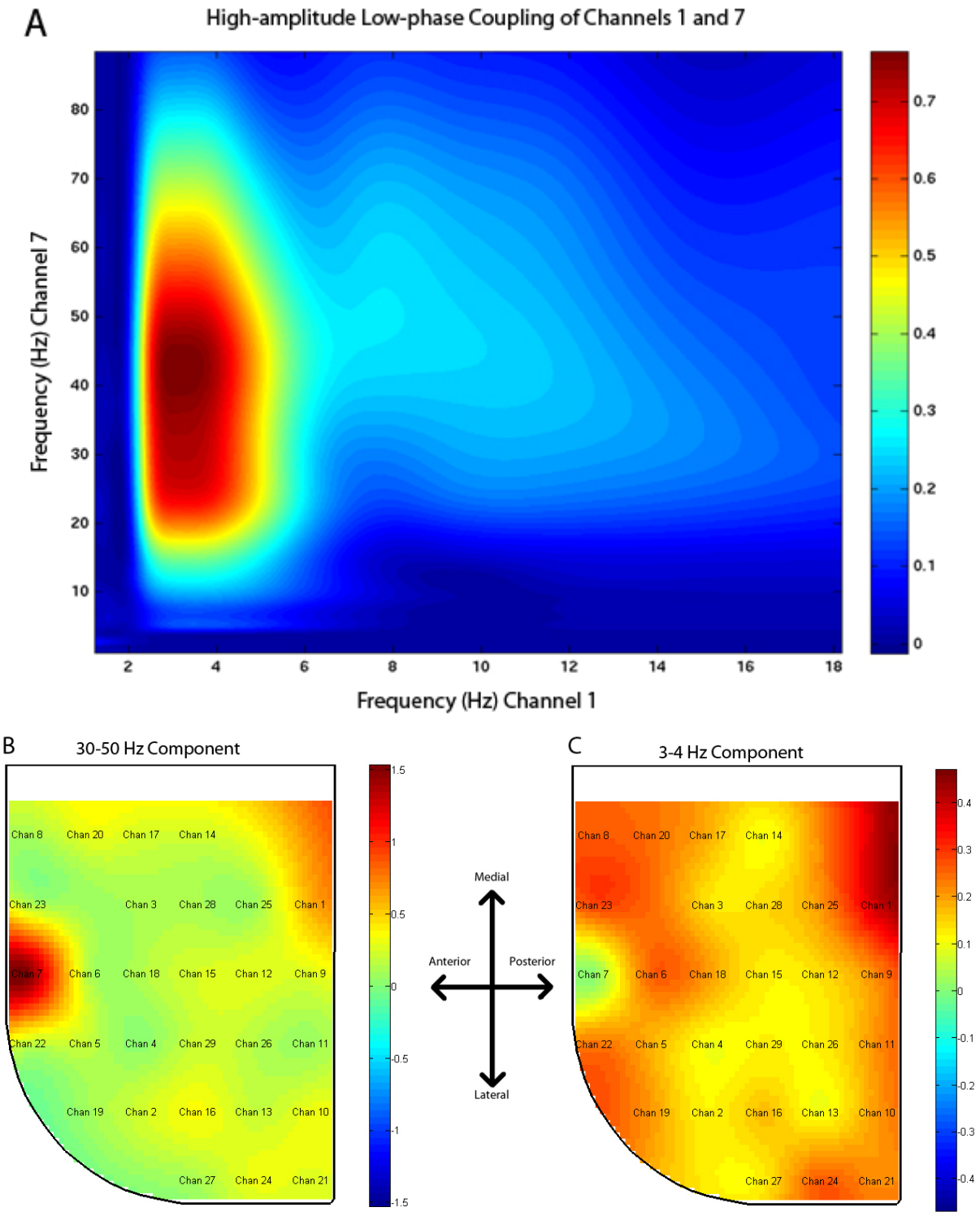

Figure 14. A) Coupling strength between the high frequency amplitude of channel 7 and the low frequency phase of channel 1. **B**) Spatial spectrum of the 30-50 Hz amplitude component **C**) Spatial spectrum of the 3-4 Hz phase component. (The scale in 14B-C represents the channel loadings of the respective components as given by the multiway model)

4. Discussion

4.1 Usefulness of the technique

The recorded data showed brain signals that were reasonably artifact-free. Furthermore, the signals obtained from different electrodes were only weakly correlated. Strong correlation was almost only found between neighbouring channels. Using these microarrays we were thus capable of recording fairly localised activity without too much common pickup due to volume conduction.

4.2 Patterns in the ongoing neurophysiological activity

The widespread coherency between lower frequencies and more localised oscillations in the higher frequency bands has been observed in several studies (Destexhe, Contreras & Steriade, 1999, in cats; Bruns & Eckhorn 2004; Maris, van Vught & Kahana, submitted, in humans). Interestingly, the tensor decomposition was able to reveal delta gamma coupling while the individual frequency components were not prominent in the frequency spectra. Moreover, most studies in rodents that have revealed couplings between frequencies found it to between hippocampal theta (4-7 Hz) and cortical gamma (e.g. Sirota et al., 2008).

We could not relate the observed oscillations to behaviour, because no behavioural task was performed. Furthermore, we expected to find more prominent spectral peaks in the delta band within the normal frequency spectra.

4.3 Future improvements

First, we are currently redesigning the shape of the recording chamber. The rat recorded from in this project probably found leverage on the posterior part of the recording chamber in order to be able to tear it off eventually. A short recording chamber should resolve this issue.

Second, the recording chamber could not be hold long enough in general. Therefore, we are currently improving the attachment of the recording chamber to the skull. Therefore,

we will pre-treat the skull area with an acidic substance before the application of the Flowline. This should roughen the bone thereby making the Flowline more adhesive to the bone.

Third, the skull bone did not heal properly. At the moment, we are testing different techniques to improve the healing process of the bone. One is to cut the lifted piece of skull into little pieces and to mix those with the TCP granules (i.e. instead of placing the whole piece back). Furthermore, we are keeping the periost intact such that we can pull it back over the refilled craniotomy; the periost is an essential part in the healing process of the bone.

Also, we are experimenting with the placement of the connector piece of the array prior to stitching. In the described technique, the connector piece was folded back over the filled craniotomy, separating the craniotomy from the skin. Now, we are trying different ways of folding the array, for instance by placing the connector piece over the jaw muscles on the contralateral side of the craniotomy. However, even though the polyimide is extremely flexible, there are limits of its possible folding.

4.3 Future behavioural experiments

During this study we have learned a lot about the behavioural capabilities of the rat and possible behavioural setups. Rats are able to learn to keep their nose in a predefined location for 5 s (i.e. to hold it still in the nose-poke hole). However, we had to constrain the movement space around the Braille cells and the nose-poke hole (remark: This is not shown in the behavioural setup depicted in this paper). This was necessary, because some rats tended to place their snout into the nose-poke hole at angles that prevent a touch of the Braille cells with the upper lip. Because we did not choose for full head constraint of the animal, there will always be some minor variability in the position of the rat, and therefore of the Braille cells. However, we consider the freedom of the rat to move around and initiate trials at his own will as being more important. Furthermore, we still have to find a method to teach the rats to distinguish between vibrotactile patterns.

In conclusion, we think that the use of polyimide microelectrode arrays will provide an excellent opportunity to chronically study large scale neural activity in the behaving rat. Especially in combination with tensor decompositions as described by Maris et al. (submitted) we are able to reveal interesting patterns of activity from multidimensional data. Unveiling these patterns will be crucial for the characterisation of the neurophysiological mechanisms of pattern recognition in the rat's somatosensory system.

Acknowledgements

I want to thank the animal caretakers Hans Krijnen and Saskia Hermeling for taking care of the animals and providing excellent support and training in handling the rats and performing the surgeries, and Elly Willems-van Bree for providing support during surgery.

Also, I want to thank Mark Hemels for building (and adjusting over and over on our request) the experimental setup, the recording chamber and the surgical equipment. A special thanks also goes to Pascal de Water and Jos Wittenbrood from the electronics group to provide soft- and hardware support, as well as for building and tweaking the electronic devices used in the experiments. Furthermore, I want to thank Maren Urner for useful discussions concerning the final manuscript.

Finally, I want to especially thank my supervisor Eric Maris for giving excellent support and guidance during the course of this project.

References

Ahissar, E. (2008). And motion changes it all. *Nat Neurosci*, *11*(12), 1369-1370.

Andersson, C. A., & Bro, R. (2000). The N-way Toolbox for MATLAB. *Chemometrics & Intelligent Laboratory Systems. 52 (1)*, 1-4.

Barrie, J. M., Freeman, W. J., & Lenhart, M. D. (1996). Spatiotemporal analysis of prepyriform, visual, auditory, and somesthetic surface EEGs in trained rabbits. *J Neurophysiol*, *76*(1), 520-539.

Benison, A. M., Rector, D. M., & Barth, D. S. (2007). Hemispheric Mapping of Secondary Somatosensory Cortex in the Rat. *J Neurophysiol*, *97*(1), 200-207.

Brecht, M., Preilowski, B., & Merzenich, M. M. (1997). Functional architecture of the mystacial vibrissae. *Behavioural Brain Research*, *84*(1-2), 81-97.

Bro, R. (1998). Multi-way Analysis in the Food Industry.

Bruns, A. (2004). Fourier-, Hilbert- and wavelet-based signal analysis: are they really different approaches? *Journal of Neuroscience Methods*, *137*(2), 321-332.

Bruns, A., & Eckhorn, R. (2004). Task-related coupling from high- to low-frequency signals among visual cortical areas in human subdural recordings. *International Journal of Psychophysiology*, *51*(2), 97-116.

Canolty, R. T., Edwards, E., Dalal, S. S., Soltani, M., Nagarajan, S. S., Kirsch, H. E., e.a. (2006). High Gamma Power Is Phase-Locked to Theta Oscillations in Human Neocortex. *Science*, *313*(5793), 1626-1628.

Cao, H., & Kuboyama, N. (In Press). A biodegradable porous composite scaffold of PGA/[beta]-TCP for bone tissue engineering. *Bone*, *In Press, Corrected Proof*.

Destexhe, A., Contreras, D., & Steriade, M. (1999). Spatiotemporal Analysis of Local Field Potentials and Unit Discharges in Cat Cerebral Cortex during Natural Wake and Sleep States. *J. Neurosci.*, *19*(11), 4595-4608.

Di, S., & Barth, D. S. (1991). Topographic analysis of field potentials in rat vibrissa/barrel cortex. *Brain Research*, *546*(1), 106-112.

Dickey, A. S., Suminski, A., Amit, Y., & Hatsopoulos, N. G. (2009). Single-Unit Stability Using Chronically Implanted Multielectrode Arrays. *J Neurophysiol*, *102*(2), 1331-1339.

Engel, A. K., Moll, C. K. E., Fried, I., & Ojemann, G. A. (2005). Invasive recordings from the human brain: clinical insights and beyond. *Nat Rev Neurosci*, *6*(1), 35-47.

Fries, P. (2009). Neuronal Gamma-Band Synchronization as a Fundamental Process in Cortical Computation. *Annual Review of Neuroscience*, *32*(1), 209-224.

Hämmerle, H., Kobuch, K., Kohler, K., Nisch, W., Sachs, H., & Stelzle, M. (2002). Biostability of micro-photodiode arrays for subretinal implantation. *Biomaterials*, *23*(3), 797-804.

Hollenberg, B. A., Richards, C. D., Richards, R., Bahr, D. F., & Rector, D. M. (2006). A MEMS fabricated flexible electrode array for recording surface field potentials. *Journal of Neuroscience Methods*, *153*(1), 147-153.

Hosp, J., Molina-Luna, K., Hertler, B., Atiemo, C. O., & Luft, A. (2009). Dopaminergic Modulation of Motor Maps in Rat Motor Cortex: An In Vivo Study. *Neuroscience*, *159*(2), 692-700.

Hosp, J. A., Molina-Luna, K., Hertler, B., Atiemo, C. O., Stett, A., & Luft, A. R. (2008). Thin-film epidural microelectrode arrays for somatosensory and motor cortex mapping in rat. *Journal of Neuroscience Methods*, *172*(2), 255-262.

Jacob, V., Le Cam, J., Ego-Stengel, V., & Shulz, D. E. (2008). Emergent Properties of Tactile Scenes Selectively Activate Barrel Cortex Neurons. *Neuron*, *60*(6), 1112-1125.

Jerbi, K., Ossandón, T., Hamamé, C. M., Senova, S., Dalal, S. S., Jung, J., e.a. (2009). Task-related gamma-band dynamics from an intracerebral perspective: Review and implications for surface EEG and MEG. *Human Brain Mapping*, *30*(6), 1758-1771.

Lakatos, P., Karmos, G., Mehta, A. D., Ulbert, I., & Schroeder, C. E. (2008). Entrainment of Neuronal Oscillations as a Mechanism of Attentional Selection. *Science*, *320*(5872), 110-113.

Maris, E., van Vugt, M., & Kahana, M. (Submitted). Multiple Neurophysiological Sources are Involved in (at least) some Patterns of Oscillatory Coupling between High-Frequency Amplitudes and Low-Frequency Phases.

Mitra, P. P., & Pesaran, B. (1999). Analysis of dynamic brain imaging data. *Biophys. J. 76*, 691-708.

Miwakeichi, F., Martínez-Montes, E., Valdès-Sosa, P. A., Nishiyama, N., Mizuhara, H., & Yamaguchi, Y. (2004). Decomposing EEG data into space-time-frequency components using Parallel Factor Analysis. *NeuroImage*, *22*(3), 1035-1045.

Molina-Luna, K., Buitrago, M. M., Hertler, B., Schubring, M., Haiss, F., Nisch, W., e.a. (2007). Cortical stimulation mapping using epidurally implanted thin-film microelectrode arrays. *Journal of Neuroscience Methods*, *161*(1), 118-125.

Molina-Luna, K., Hertler, B., Buitrago, M. M., & Luft, A. R. (2008). Motor learning transiently changes cortical somatotopy. *NeuroImage*, *40*(4), 1748-1754.

Mörup, M., Hansen, L. K., Herrmann, C. S., Parnas, J., & Arnfred, S. M. (2006). Parallel Factor Analysis as an exploratory tool for wavelet transformed event-related EEG. *NeuroImage*, *29*(3), 938-947.

Paxinos, G., & Watson, C. (2007). *The Rat Brain in Stereotaxic Coordinates* (Sixth Edition.). Amsterdam: Elsevier.

Petersen, C. C. (2007). The Functional Organization of the Barrel Cortex. *Neuron*, *56*(2), 339-355.

Percival, D. B., & Walden, A. T. (1993). *Spectral analysis for physical applications.* Cambridge: Cambridge University Press.

Rodgers, K. M., Benison, A. M., Klein, A., & Barth, D. S. (2008). Auditory, Somatosensory, and Multisensory Insular Cortex in the Rat. *Cereb. Cortex*, *18*(12), 2941-2951.

Rubehn, B., Bosman, C., Oostenveld, R., Fries, P., & Stieglitz, T. (2009). A MEMS-based flexible multichannel ECoG-electrode array. *J. Neural Eng. 6.*

Schanze, T. & Eckhorn, R. (1997). Phase correlation among rhythms present at different frequencies: spectral methods, application to microelectrode recordings from visual cortex and functional implications. *Int. J. Psychophysiol., 26(1-3),*171-89

Shlens, J. (2009). A Tutorial on Principal Component Analysis. Retrieved (22-4-2009) from: http://www.snl.salk.edu/~shlens/notes.html.

Sirota, A., Montgomery, S., Fujisawa, S., Isomura, Y., Zugaro, M., & Buzsáki, G. (2008). Entrainment of Neocortical Neurons and Gamma Oscillations by the Hippocampal Theta Rhythm. *Neuron*, *60*(4), 683-697.

Taylor, K., Mandon, S., Freiwald, W. A., & Kreiter, A. K. (2005). Coherent Oscillatory Activity in Monkey Area V4 Predicts Successful Allocation of Attention. *Cereb. Cortex*, *15*(9), 1424-1437.

Varela, F., Lachaux, J., Rodriguez, E., & Martinerie, J. (2001). The brainweb: Phase synchronization and large-scale integration. *Nat Rev Neurosci*, *2*(4), 229-239.

von Stein, A., Chiang, C., & König, P. (2000). Top-down processing mediated by interareal synchronization. *Proceedings of the National Academy of Sciences of the United States of America*, *97*(26), 14748-14753.

Ward, M. P., Rajdev, P., Ellison, C., & Irazoqui, P. P. (2009). Toward a comparison of microelectrodes for acute and chronic recordings. *Brain Research*, *1282*, 183-200.